

Toward the Synthesis of the Deuterated Finland Trityl Radical

A Seniors Honors Thesis

Presented in Partial Fulfillment of the Requirements for graduation *with research distinction* in Chemistry in the undergraduate colleges of The Ohio State University

By

Caitlin A. Wenzke

The Ohio State University  
June 2009

Project Advisor: Professor Christopher Hadad, Department of Chemistry

CERTIFICATION FOR GRADUATION *WITH RESEARCH DISTINCTION*

TO: The Colleges of the Arts and Sciences Honors Committee

DATE OF EXAMINATION: MAY 29, 2009This is to certify that CAITLIN WENZKE

has completed successfully the required examination for graduation (check one):

☒ *with research distinction in* (major field) CHEMISTRY☐ *with research distinction* (for thesis outside the major field)and the judgment of the examination committee is that the quality of all written and oral work is such that the candidate should be graduated *with research distinction*.

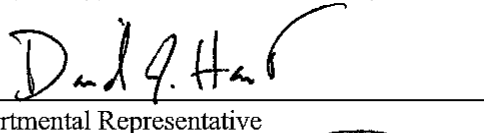
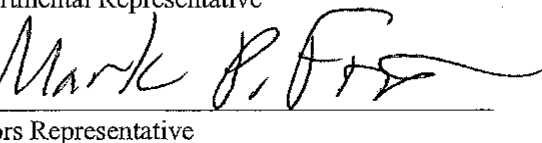
With the signatures of all three examination committee members, the committee further certifies that the candidate has successfully defended the thesis during a one-hour oral examination before its three members and that the candidate has met any additional departmental requirements.

THESIS TITLE: SYNTHESIS TOWARD  
DEUTERATED FINLAND  
TRITYL RADICAL

## SIGNATURES OF COMMITTEE MEMBERS

Printed or typed name:

Signature:

CHRISTOPHER HADAD  
Project Advisor  
Project AdvisorDAVID HART  
Departmental Representative  
Departmental RepresentativeMARK FOSTER  
Honors Representative  
Honors Representative

Note: Please return one copy of this certification to the ASC Honors Office, 207 Enarson Hall. You may want to keep a copy for your records as well.

## Acknowledgements

I would like to first thank Dr. Christopher Hadad for allowing me to join his research group so that I may apply the knowledge I have acquired the past few years as a Chemistry major. I am really grateful for the motivation he instilled in me to obtain the most from my undergraduate research experience. Participating in the undergraduate research forums and writing and defending this senior thesis all required a lot of hard work, but were very rewarding. Thank you very much for all your help.

I would also like to thank Dr. Arthur Winter for all of his assistance with my research the past year. He was always there for me both inside and outside the laboratory, and I greatly appreciate all that he has done for me. He is truly a “pioneer” and will be deeply missed by the Hadad group.

Lastly, I would like to thank the rest of the Hadad group members for all of their help. Even though they were not directly involved in my project, they were always willing to help. I will miss seeing all of you and wish you the best of luck in each of your future endeavors.

## Table of Contents

Acknowledgements	iii
I: Electron Paramagnetic Resonance Imaging: Introduction	1
II: Synthesis of a Deuterated Trityl Radical	18
III: Methods	24
Works Cited	29

## Electron Paramagnetic Resonance Imaging

## Introduction

Magnetic resonance imaging (MRI) has become a widespread technique for full-body imaging.<sup>1</sup> MRI machines operate in a similar manner to nuclear magnetic resonance (NMR) instruments, with the principle difference being that MRI exploits a gradient in the external magnetic field across a much larger sample to obtain three-dimensional images. MRI machines contain a cavity for the patient surrounded by a large electromagnet (see Figure 1-1).<sup>2</sup> The strong external magnetic field produced by this magnet acts to break nuclear spin degeneracies (arbitrarily labeled  $\alpha$  and  $\beta$ ) in the tissue of the patient. Radiofrequency light is then irradiated on the patient, and radiofrequencies with the precise energy required to flip an  $\alpha$  spin into a  $\beta$  spin are absorbed. Since the intensities of these absorbances are related to the nuclei density, a three-dimensional image mapping nuclei concentration can be generated. For example, a common technique is to map the intensity of  $^1\text{H}$  (proton) absorption of water molecules in order to give a

three-dimensional image of the water concentrations in the body. This image can distinguish certain abnormal sites from healthy tissues, since different tissue types have different concentrations of water.

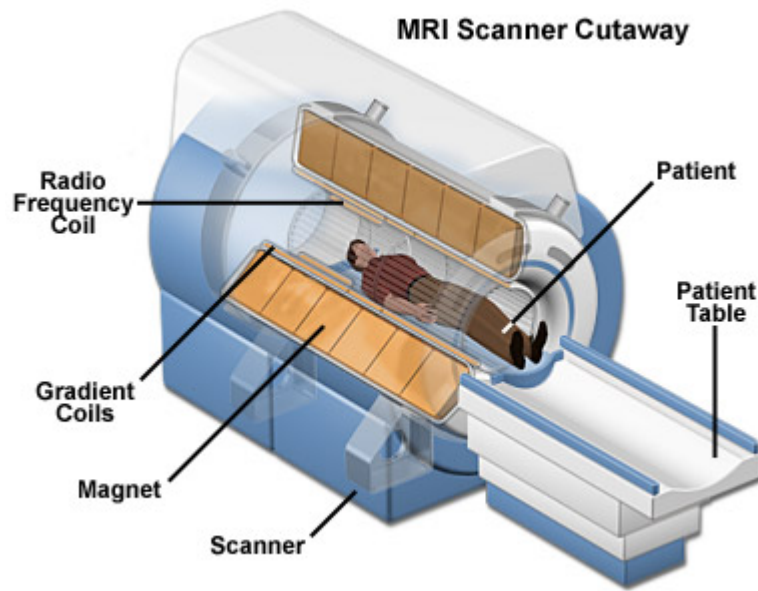


Figure 1-1: MRI machine<sup>2</sup>

MRI has been developed extensively over the years and can be used to study humans because of the prevalence of protons in soft tissue and water as well as their long relaxation times.<sup>3</sup> Using an MRI image, such as the one depicted in Figure 1-2, physicians can determine that the patient has a brain tumor as indicated by the white area in the lower left-hand-side of the figure. These three-dimensional images are obtained non-invasively and can be used to diagnose a variety of pathological conditions and, more recently, to obtain functional information.<sup>3</sup> NMR detects  $^1\text{H}$ ,  $^{31}\text{P}$ ,  $^{13}\text{C}$ , and other nuclei with non-zero nuclear spin, just as is possible with NMR, providing a number of different avenues for distinguishing diseased tissues from healthy.<sup>1</sup>

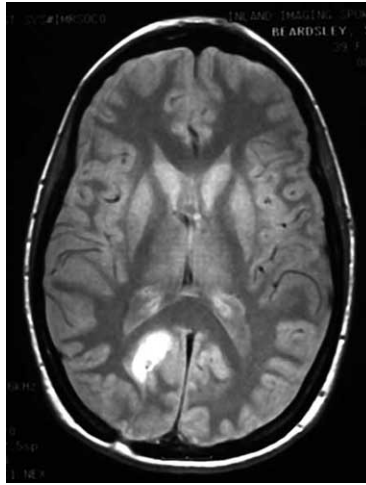


Figure 1-2: MRI image<sup>4</sup>

A related technique to MRI is electron paramagnetic resonance imaging (EPRI). This technique is becoming increasingly popular and also utilizes applied magnetic gradient fields. Unlike NMR, EPR is used to detect any species with unpaired electron spin. Thus, while NMR involves the excitation of nuclear spin, EPR involves the excitation of unpaired electronic spins.<sup>1</sup> EPR can therefore detect, in principle, any open-shell species that has unpaired electrons including doublet radicals (e.g. nitric oxide, NO), triplet diradicals (e.g. molecular oxygen,  $^3\text{O}_2$ ), and other reactive oxygen species in biological systems.<sup>5</sup>



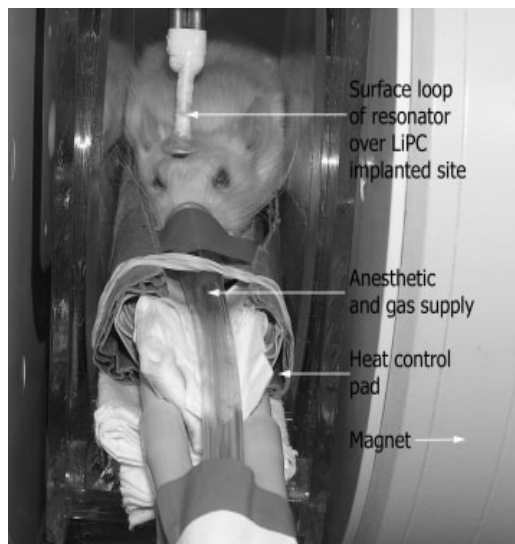


Figure 1-3: EPR machine<sup>6</sup>

Electron Paramagnetic Resonance Imaging (EPRI) is, likewise, very similar to MRI. EPRI only detects species with unpaired spin, leading to a decrease in background noise compared to MRI because few biological species have unpaired electrons. This technique likewise allows for *in vivo* imaging, which can provide biochemical, physiological, and pharmacological information on animals without euthanizing the test animals. Many other methods require that the small animals, usually mice, be euthanized in order for the tissues to be examined. EPRI may significantly improve biomedical research by allowing information to be collected without risking the life of the animals. In the future, EPRI will also hopefully be able to be applied to the study of humans.<sup>1</sup> Figure 1-3 shows a typical EPRI machine containing a mouse.<sup>6</sup>

While EPRI can, in principle, directly monitor important biological radicals such as nitric oxide, triplet oxygen ( $^3\text{O}_2$ ), as well as reactive oxygen and nitrogen species; in practice, EPRI requires the use of exogenous compounds to permit this imaging. The

small amounts of paramagnetic species present in organisms, the spin-spin relaxation of triplet diradicals (such as  $^3\text{O}_2$ ), as well as the short-lived nature of these intermediates impairs direct imaging. For example, diamagnetic spin traps that become stable paramagnetic species upon reaction with the species of interest (such as a member of the class of reactive oxygen species) can be exploited as a way to indirectly image the concentration of the species of interest. Alternatively, paramagnetic probes that have their EPR signal altered by pH or upon collision with the species of interest can be employed. For example, stable radical probes can indirectly measure oxygen concentrations because collisions of the exogenously injected radical with paramagnetic oxygen lead to broadening of the radical signal.<sup>5</sup> The signal's line width can be used to elucidate a measurement of the oxygen concentration at that particular site to form a three-dimensional image of oxygen concentrations over a body.

EPRI probes must meet a number of requirements, including that they be water soluble, stable in biological systems, nontoxic, have a pharmacological half-life that allows imaging in at least ten minutes, and produce a narrow and intense signal (ideally a singlet peak) in the EPR spectrum.<sup>1</sup> Use of EPRI has been limited by the small amount of endogenous free radicals, the lack of ideal spin probes, short relaxation times, and slow acquisition of data. Moreover, previous spin probes suffered from undesirable properties of toxicity, poor signal monodispersity, and very short relaxation times. Two families of spin probes that have been developed that exhibit these characteristics are nitroxide radicals and trityl radicals. These two classes of radical can be injected into the organism, eliminating the need for less desirable invasive methods.<sup>5</sup>

Images of a mouse brain in Figure 1-4<sup>6</sup> were obtained using EPRI and a triarylmethyl (trityl) radical as the spin probe. Collection of the EPR spectrum at each pixel (plot C), allows different images to be made that plot different features contained in the spectra. Figure A plots the intensity of the signal at each point, which can be used to show the rough distribution of the tag. The white area is the area of high intensity (high tag concentration), while the gray area is the area of low intensity (low concentration). B plots the line width of the signal in C, with dark blue spots indicating a broader line width and light blue a more narrow line width.<sup>6</sup> Since the line width is proportional to the oxygen concentration, this image can be used as an indirect way of imaging oxygen concentrations (described in more detail *vide infra*).

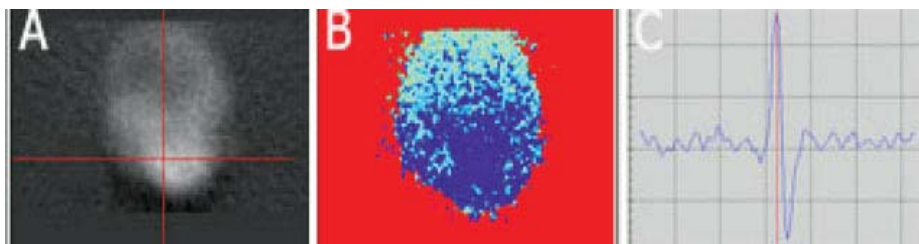


Figure 1-4: EPR Imaging of mouse brain using triarylmethyl radical<sup>6</sup>

Nitroxyl radicals and triarylmethyl (trityl) radicals are both part of a class of probes known as soluble probes – those that are soluble in biological media. These radicals can be used to measure dissolved O<sub>2</sub> concentration. An example of a soluble probe, a triarylmethyl radical, can be seen in Figure 1-5b. The other class of probes, such as particulate probes, includes lithium phthalocyanine, naturally occurring coal, and synthetic char. Lithium phthalocyanine probes are shown in Figure 1-5a. Particulate

probes can be used to measure oxygen partial pressure, but they have a significant disadvantage, namely that these probes must be surgically inserted into tissues.<sup>5</sup>

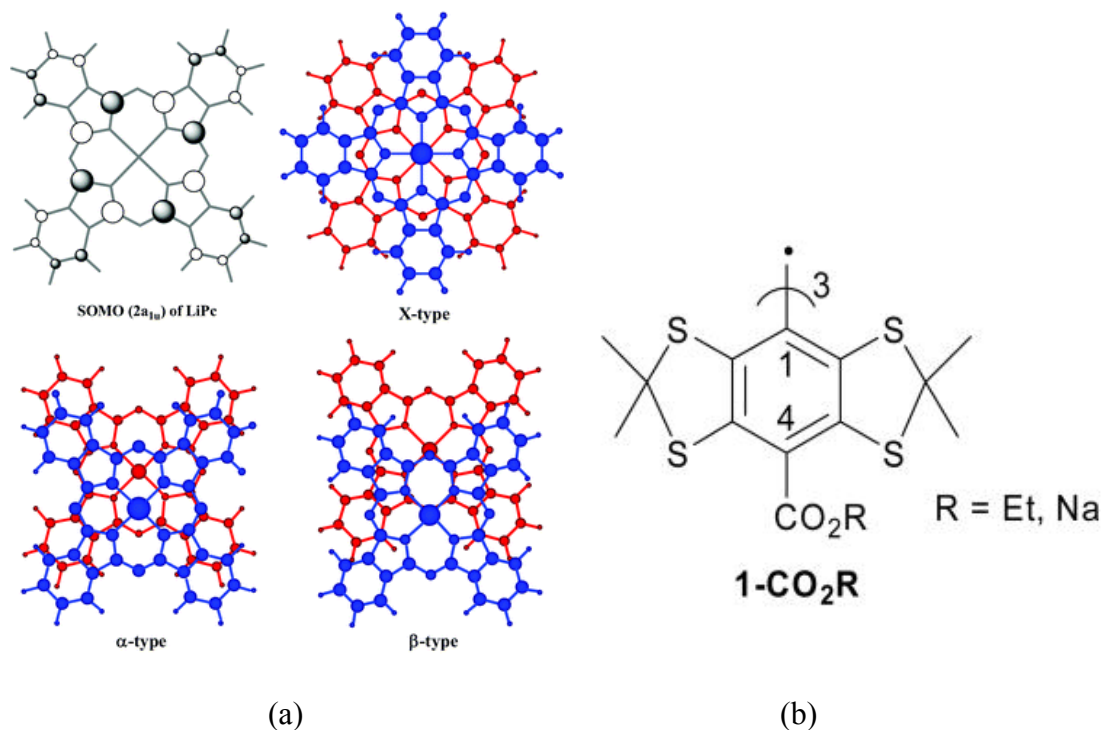


Figure 1-5: (a). Lithium phthalocyanine, a particulate probe; (b). Tetrathiatriarylmethyl (trityl, TAM) radical, a soluble probe.

A focus of the Hadad group has been on developing soluble EPRI probes, in particular, the tetrathiatriarylmethyl (TAM) radical as shown in Figure 1-6. TAM radicals have four sulfur atoms on the phenyl ring, and, just like other trityl radicals, the unpaired electron is situated at least four atoms lengths away from the methyl carbon. This design removes the possibility for other hydrogen atoms on the molecule to couple with the radical and cause broadening of the signal or multiple hyperfine coupling (splitting).<sup>7</sup> The

sulfur atom, having two lone pairs of electrons, also helps by shielding the radical species.<sup>8</sup>

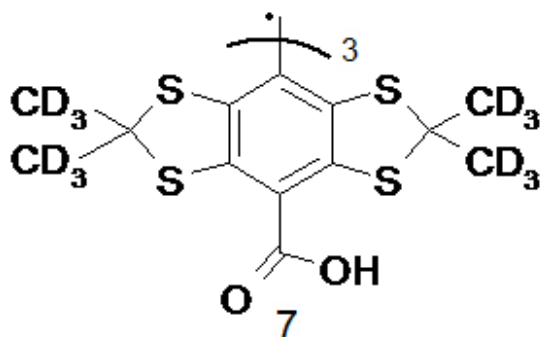


Figure 1-6: The TAM radical being synthesized by the Hadad group

Trityl radicals have advantages over nitroxyl radicals, including high signal sensitivity, stability in cells and tissues, and flexibility to independently measure the concentration of superoxide radical anion and  $O_2$  by EPR signal loss and line broadening, respectively.<sup>9</sup> Furthermore, the trityl radical serves as an excellent spin probe because it is water soluble and produces a narrow and sharp singlet signal in the EPR spectrum ( $<100$  mG).<sup>9</sup> The probe creates a single narrow line in the EPR spectrum because no magnetic nuclei are close to the unpaired electron on the molecule.<sup>1</sup> The radical is stable because it is tri-substituted and, thus, the spin density is delocalized over three rings.<sup>9</sup> The toxicity of the spin probes is negligible and, therefore, tolerated in small animals. The half life of these spin probes ranges from ten to twenty minutes, making them ideal for collecting images.<sup>1</sup>

A goal of the Hadad group is to develop improved probes through the synthesis of a deuterated version of a trityl radical in which the  $\text{CH}_3$  groups are replaced by  $\text{CD}_3$  units. Deuterated and protiated versions of this trityl radical probe can be seen below in Figure 1-7. Even though there is no direct coupling of the unpaired electron with the hydrogens or deuteriums, the number of hydrogens on the methyl group does affect the width of the EPR singlet – being a narrow peak for the deuterated TAM radical. Moreover, one can also replace the carboxyl group ( $-\text{CO}_2\text{H}$ ) on each phenyl ring of the TAM radical with a hydrogen, which results in a doublet (two peaks) in the EPR signal, whereas having two hydrogens can increase the number of signals to a triplet.<sup>9</sup> Hadad and co-workers synthesized the non-deuterated version in the past, but the drawback of the non-deuterated version is that the peak width in the EPR spectrum is broader for the non-deuterated version. Figure 1-8 shows how a change in pH affects the line width as a consequence of coupling of the electron spin with the nuclear spin of the hydrogen. As the pH is lowered, more of the radicals become protonated and the signal broadens.<sup>10</sup>

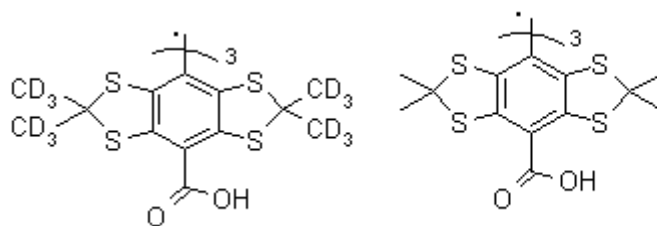


Figure 1-7: Two types of trityl radicals; the deuterated version on the left and the non-deuterated version of the same probe on the right

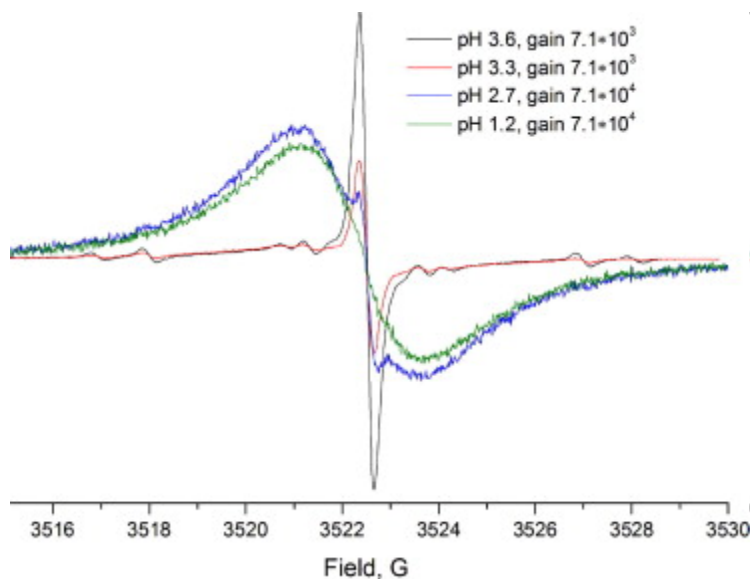


Figure 1-8: The effect of pH on the line width of the EPR spectrum<sup>10</sup>

The paramagnetic spin probe can be used to measure oxygen levels because of EPR line broadening. Molecular oxygen, which has two unpaired electrons in its ground state, undergoes a spin exchange interaction with the paramagnetic EPR spin probe, causing a broadening of the EPR line as seen in Figure 1-9.<sup>11</sup> According to the Smoluchowsky Theory, the line-width is directly proportional to oxygen concentration.<sup>5</sup> A graph of this relationship can be seen in Figure 1-10.<sup>10</sup>

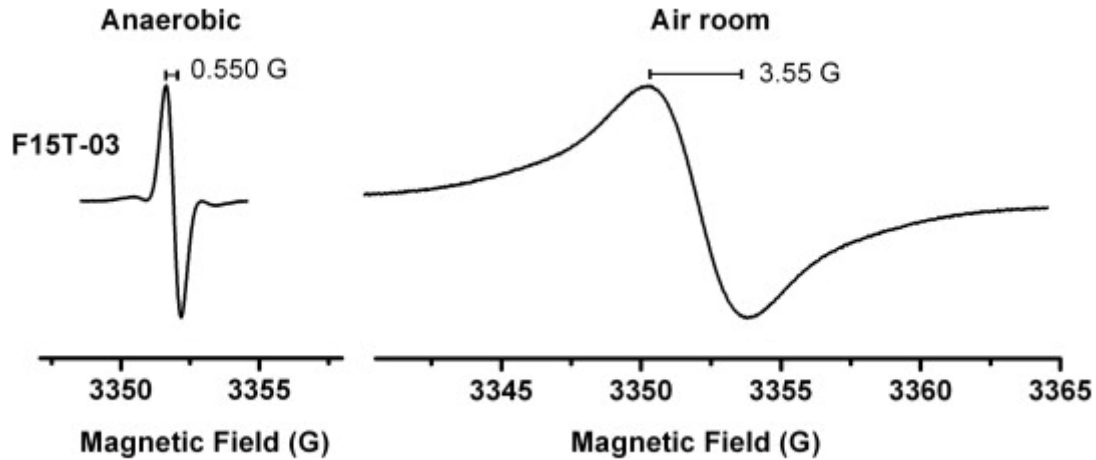


Figure 1-9: The effect of oxygen on the line width of the EPR spectrum can be seen when comparing these two graphs. In the right graph, one can see that being in the air and, hence being exposed to oxygen, broadens the line width.<sup>11</sup>

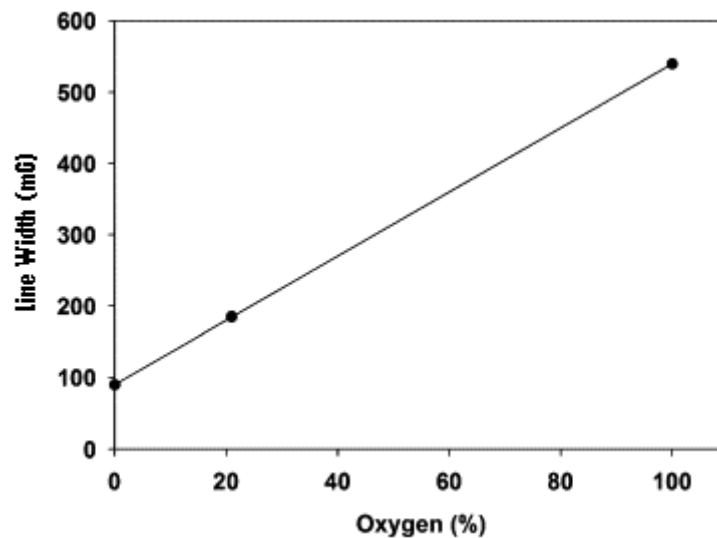


Figure 1-10: Dependence of the EPR line width on the amount of oxygen present<sup>10</sup>

EPR oximetry, the measurement of oxygen in the blood using EPR, can be used to understand the roles of oxygen in living organisms.<sup>8</sup> The exact role of oxygen in living cells is unknown. Cells require oxygen to produce metabolic energy, but the amount of oxygen thought to be required varies.<sup>12</sup> EPRI has been used in rats to study the dynamic



changes in oxygen concentration in the body as a function of time (see Figure 1-11).<sup>13</sup> The highest concentration is seen in the kidneys of the rats because the rat is trying to excrete the spin probe that has been injected into its body.<sup>13</sup> This method will be particularly useful for developing a clinical diagnostic to distinguish treatments for patients, especially in cancer cells for which the  $pO_2$  is low.<sup>8</sup>

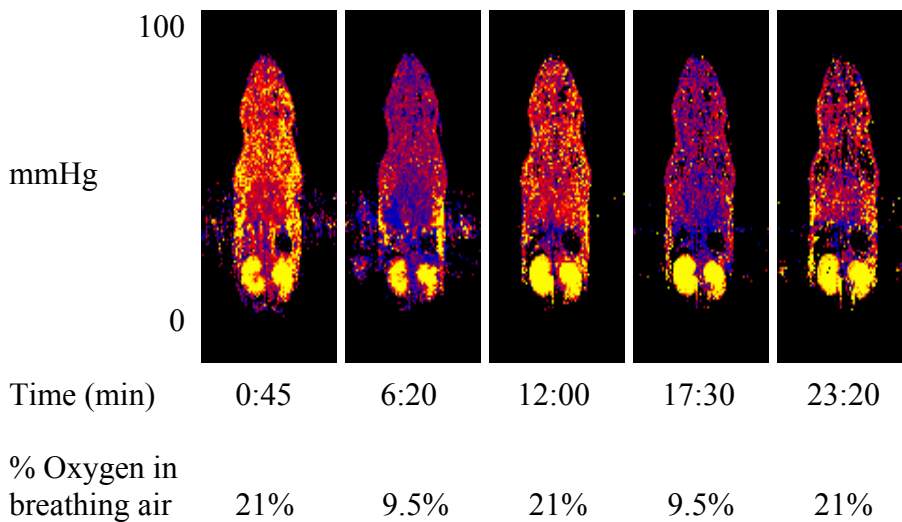


Figure 1-11: The distribution of oxygen in a rat over time, with yellow areas showing the highest concentration of oxygen.<sup>13</sup>

As a consequence of the unchecked growth of tumors, oxygen levels in cancer cells are lower than in normal cells before tumors can recruit their vascular network and blood supply. The abnormalities in the tumor vessels lead to irregular and sluggish blood flow, resulting in low  $O_2$  delivery,<sup>3</sup> as seen in Figure 1-12b. This hypoxia can lead to tumor proliferation and malignant progression because tumor cells can learn to successfully adapt to this low oxygen environment. The genomic changes include point mutations (insufficient DNA repair, errors in DNA replication, or both), chromosomal

rearrangements, and gene amplification. The changes activate angiogenesis, anaerobic metabolism, and other processes that help tumor cells survive and proliferate. Since these adapted cells are the ones surviving and proliferating, they will become the dominant cell in the tumor and will have the characteristics necessary for metastasizing, or spreading, to other nearby tissues.<sup>3</sup>

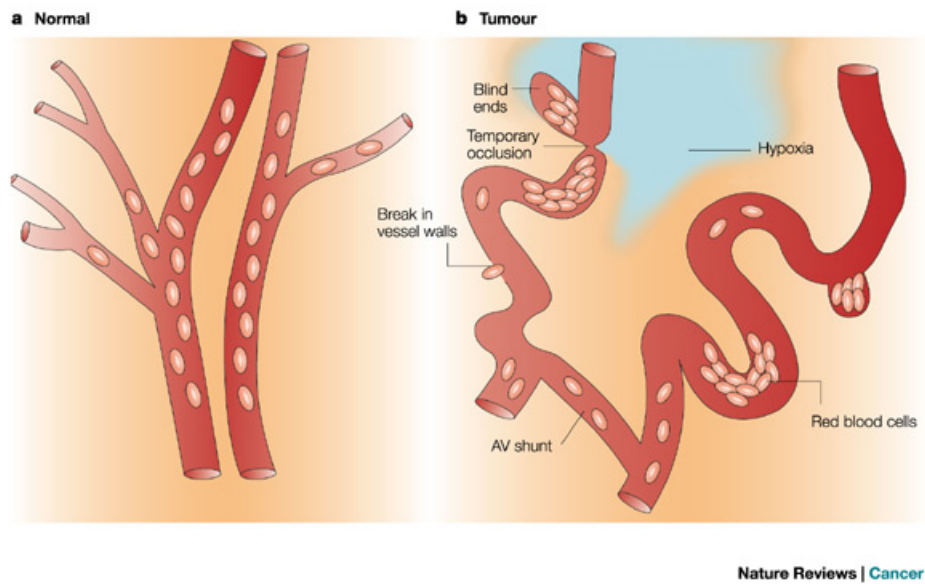


Figure 1-12: (a) Normal vessels; (b) Tumor vessels with irregular and sluggish blood flow (low  $O_2$  delivery)<sup>14</sup>

Hypoxia is also thought to affect how well cancer treatments, such as radiation and chemotherapy, work. If the level of oxygen in the tumor influences the effectiveness of certain cancer treatments, it would be important to know the level of  $pO_2$  before selecting the appropriate cancer treatment and to determine a method for improving the tumor hypoxia.<sup>3</sup> Information about the level of  $pO_2$  can be determined through the use of EPRI and spin probes.

The deuterated Finland (tetrathiatriarylmethyl, TAM) trityl radical being produced by Hadad et al. will be used to monitor the oxygen concentration in living cells. The type of spectroscopy utilized is proton-electron paramagnetic double resonance imaging (PEDRI) spectroscopy. PEDRI is a technique used to measure the spatial distribution of free radicals in biological samples and small animals and can be used in vivo or ex vivo.<sup>15</sup> This technique is based on the Overhauser effect, which causes the EPR resonance of the paramagnetic species to be irradiated while collecting the NMR image.<sup>16</sup>

PEDRI has many advantages and disadvantages. It has good sensitivity, high spatial resolution that does not depend on the line width of the free radicals, and the capacity to rapidly acquire images. Unlike EPRI, PEDRI also does not require the use of very strong magnetic field gradients and should be able to produce images in an even shorter time than EPRI. One disadvantage of PEDRI spectroscopy is that the microwave irradiation required to flip an electron in EPR can result in overheating of the biological sample as a consequence of background absorption of the microwaves by water.<sup>17</sup>

Like EPRI, PEDRI can also utilize trityl radicals and produce images of the free radical distribution in living organisms. Using PEDRI, the distribution of the TAM probe has been studied in mice, such as the mouse in Figure 1-13, in which the heart, major vessels, kidneys, and bladder can be seen. The intensity of the image at each of these locations was plotted as a function of time in Figure 1-14. Information can be obtained from this graph about the distribution and clearance of the TAM probe. Initially, the

probe is found to be in the heart, lungs, and large vessel locations. The probe is eventually taken up by the kidneys and, later, excreted to the bladder. This information can be used to study perfusion, oxygenation and other important parameters in humans. Eventually, image quality and acquisition speed should be improved.<sup>15</sup>

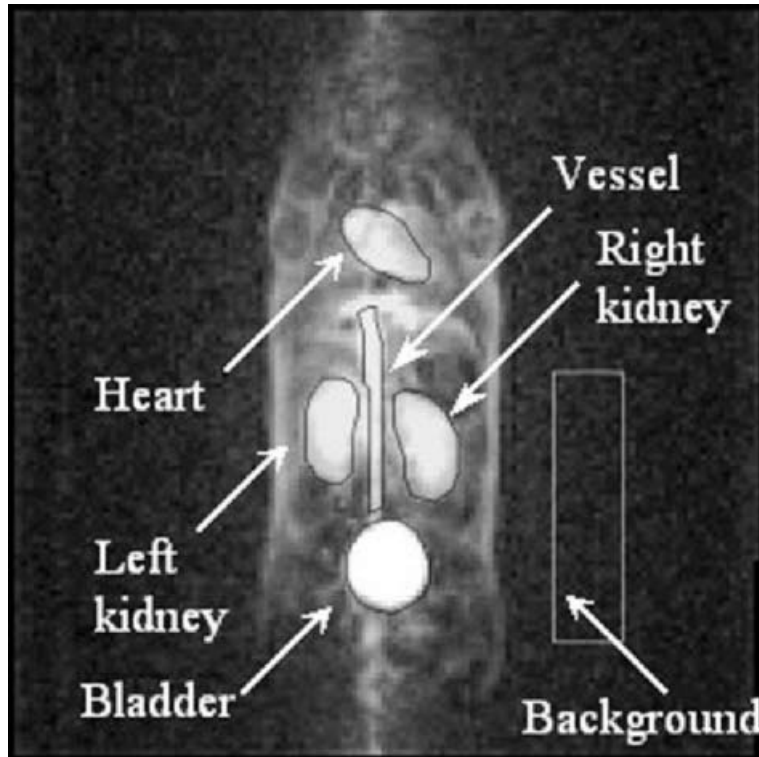


Figure 1-13: Image using PEDRI and TAM probe<sup>15</sup>

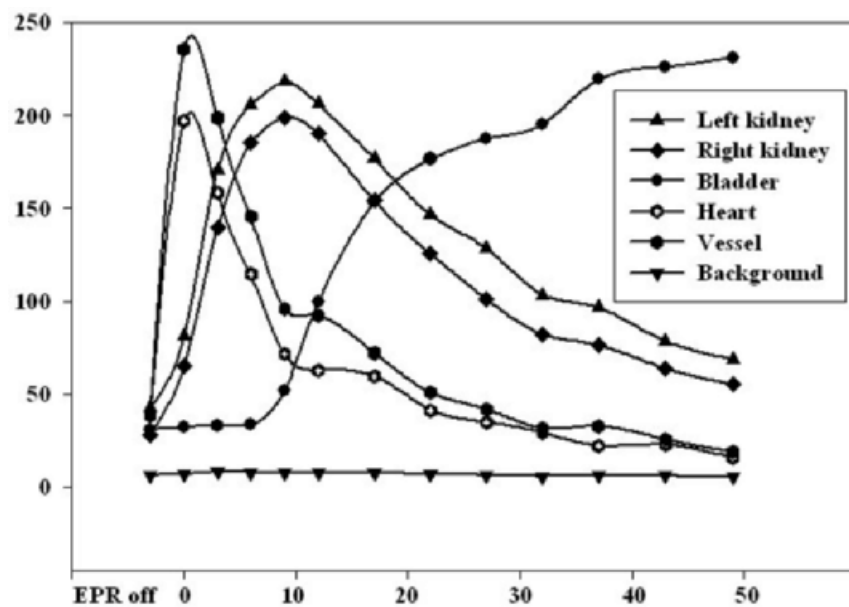


Figure 1-14: Intensity of image at location as a function of time.<sup>15</sup>

## II

## Synthesis of a Deuterated Trityl Radical

### Synthesis of a Deuterated Tetrathiatriarylmethyl Radical

During the past year, the Hadad group has sought to synthesize a deuterated tetrathiatriarylmethyl (trityl) radical for use in electron paramagnetic resonance imaging (EPRI) spectroscopy, a procedure used to monitor the oxygen concentration in living cells. The synthesis involves six steps (see Figure 2-1). Reddy et al. performed a similar procedure for the non-deuterated compound, and this procedure was modified in order to synthesize the deuterated compound.<sup>8</sup> Thus far, we have successfully accomplished the first three steps of the synthesis. Difficulties remain in scaling up the second step of the synthesis and finding appropriate conditions for optimizing the third step.

The first step (step 1 of Figure 2-1) has been attempted three times in order to obtain more starting material: 1,2,4,5-tetra-*tert*-butylthiobenzene. The solubility of the product was checked in many solvents for purification by recrystallization. A good solvent for recrystallization allows the product to be insoluble at low temperature and

soluble at high temperature. The product was found to be insoluble in acetone at low temperature and soluble in acetone at high temperature. After the product was dissolved in acetone at high temperature, it was recrystallized at room temperature. Acetone was used for the recrystallization step because it was the best solvent in these initial solubility tests.

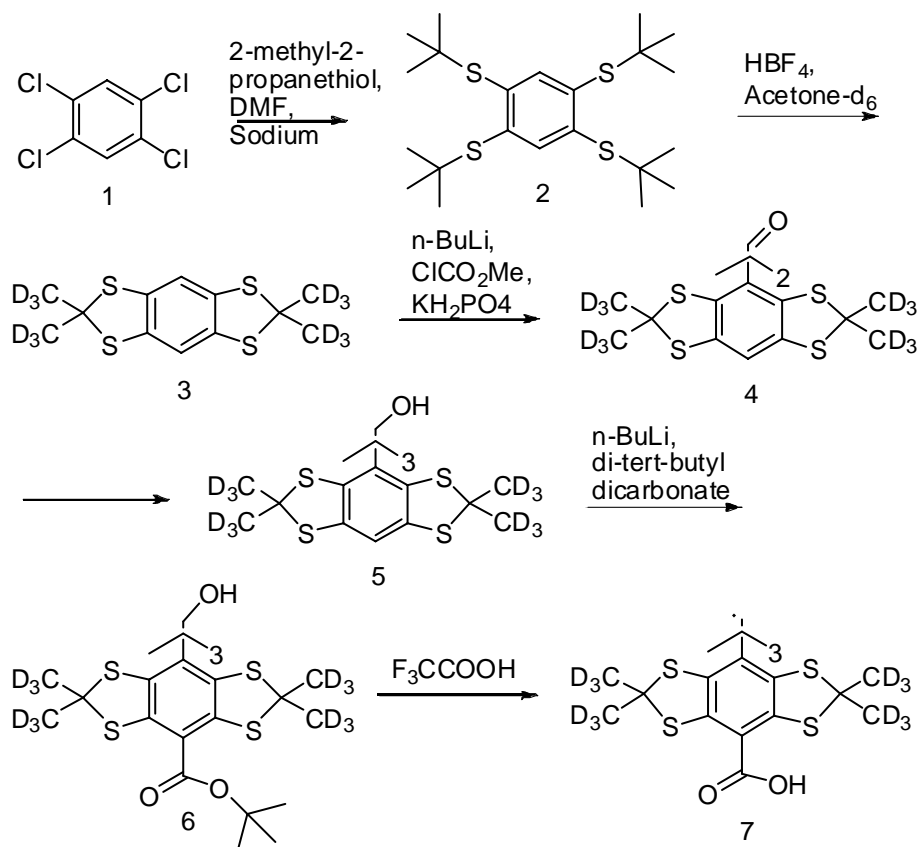


Figure 2-1: Synthesis scheme for the deuterated trityl radical

**1,2,4,5-Tetra-*tert*-butylthiobenzene.** 2-methyl-2-propanethiol (39 mL) was put under Ar for five minutes. Dry DMF (200 mL) was then added. The reaction was stirred over ice ( $0^\circ\text{C}$ ) and then sodium (8.100 g), cut into small chunks, was added. The reaction was allowed to reach room temperature and then stirred overnight for 21 hours. 1,2,4,5-



Tetrachlorobenzene (14.705 g) was then added to the reaction, and the reaction was then refluxed (120°C) under argon for 23 hours. After the reaction was taken off reflux and cooled to room temperature, the reaction was poured over ice (200 g). The precipitate was removed by vacuum filtration, washed with cold water, and dried on house vacuum overnight (23 hours) to yield an off-white powder (21.74 g). Recrystallization of the product was then performed using acetone, and the product from the recrystallization was dried on house vacuum for approximately 2.5 days to give an off-white, tan powder:  $^1\text{H}$  NMR (250 MHz,  $\text{CDCl}_3$ )  $\delta$  1.3 (s, 12 H), 7.94 (s, 2H).

The second step of the reaction has been performed 28 times in an attempt to optimize the reaction yield and the percent deuteration of the product. These attempts can be seen in Table 2-1. Attempt 3, the attempt with the highest percent deuteration, is described in detail in the next paragraph. The majority of the attempts are performed using toluene as the solvent. Since  $\text{BF}_3$  from the acid ( $\text{HBF}_4$ ) could have removed protons from toluene and formed a non-deuterated product, other solvents and additives were tested, including nitrobenzene,  $\text{DCI}$ , and benzene- $\text{d}_6$ . Changing the equivalents of acid and deuterated acetone was also tried to increase the percent deuteration. The reaction did not work as successfully when these equivalents were changed. In addition, efforts were made to dry the reaction mixture to prevent water from interfering with the reaction and adding hydrogens to the mixture. These efforts included using 3 Å molecular sieves, purging the reaction with argon, and using a Dean-Stark trap to distill off water. None of these experiments helped to increase the percent deuteration and were abandoned. To optimize the conditions of step 3, the synthesis of the non-deuterated product was also performed.

Attempt	Equivalents Starting Material	Equivalents Acetone-d <sub>6</sub>	Equivalents HBF <sub>4</sub>	Solvent (special condition)	Percent Deuteration
1	1	2	(10 NaBF <sub>4</sub> )	DCI/Et <sub>2</sub> O	No rxn
2	1	2	1	Toluene	No rxn
3	1	2	1	Toluene	92
4	1	2	1	Toluene	50
5	1	2	1	Toluene	80-85
6	1	2	(0.5 BF <sub>3</sub> /DCI)	Toluene	80
7	1	2	1	Nitrobenzene	80-85
8	1	2	1	Benzene	80-85
9	1	2	1	Benzene-d <sub>6</sub>	80-85
10	1	10	0.5	Toluene	No rxn
11	1	10	1	Toluene	No rxn
12	1	6	1	Toluene	No rxn
13	1	2	1	Toluene (purged)	~0
14	1	2	1	DCI, Toluene (purged)	79
15	1	2	1	Benzene-d <sub>6</sub>	No rxn
16	5	10	5	Toluene	No rxn
17	5	10	5	Toluene (Dean-Stark trap)	79
18	10	20	10	Toluene	No rxn
19	10	20	10	Toluene	No rxn
20	10	(20 acetone)	10	Toluene (sieves)	No rxn
21	8	(3.2 acetone)	20	Toluene	N/A
22	20	0.4	20	Toluene	No rxn
23	5	2	1	Toluene (sieves)	No rxn
24	1	2	1	Toluene	
25	1	2	1	Toluene	
26	10	20	10	Toluene	No rxn
27	5	10	5	Toluene	No rxn
28	2.5	5	2.5	Toluene	

Table 2-1: Attempts with step 2 (see Figure 2-1) of the deuterated trityl radical synthesis.

**2,2,6,6-Tetramethylbenzo[1,2-*d*;4,5-*d*]bis[1,3]dithiole. Method A (Attempt 3).**

1,2,4,5-Tetra-*tert*-butylthiobenzene (0.1002 g) was added to a round bottom flask. Acetone- $d_6$  (0.35 mL), 54%  $\text{HBF}_4$  in ether (0.05 mL), and a stir bar were then added. The reaction was stirred at room temperature for thirty minutes. Diethyl ether (1.0 mL) was then added to prevent drying of the reaction mixture. The reaction was continuously stirred at room temperature for two additional hours. Toluene (0.95 mL) was then added to the reaction, and the temperature of the reaction mixture was increased to  $120^\circ\text{C}$ , then allowed to reflux for approximately 2.5 days. The resulting black mixture was then cooled to room temperature and treated with saturated aqueous  $\text{NaHCO}_3$  (20 mL). The crude product was extracted with ether (2 x 25 mL).  $\text{MgSO}_4$  was used to dry the combined extracts, which were then concentrated in vacuo to yield a pale yellow solid.

$^1\text{H}$  NMR (250 MHz,  $\text{CDCl}_3$ )  $\delta$  1.82 (s, 12H), 6.999 (s, 2H).

### III

#### Methods

## Methods

Synthesis of the deuterated trityl radical requires the use of deuterated compounds, including acetone-d<sub>6</sub> and benzene-d<sub>6</sub>. An acid, HBF<sub>4</sub>, NaBF<sub>4</sub>/DCI, or BF<sub>3</sub>/DCI is also required. Many solvents and additives are used, including toluene, diethyl ether, DCI, and nitrobenzene. These solvents are bought from Aldrich and were not purified further, with the exception of nitrobenzene, which was distilled.

The reactions were checked for completion by using thin layer chromatography (TLC, see Figure 3-1).<sup>18</sup> Aluminum-backed silica gel plates were used for TLC. The solvent used is 98% hexanes: 2% ethyl acetate. Three spots are made on the plates of starting compound, product, and both. The reaction is determined to be complete when the starting material is no longer present in the product. At this point, the reaction was stopped.

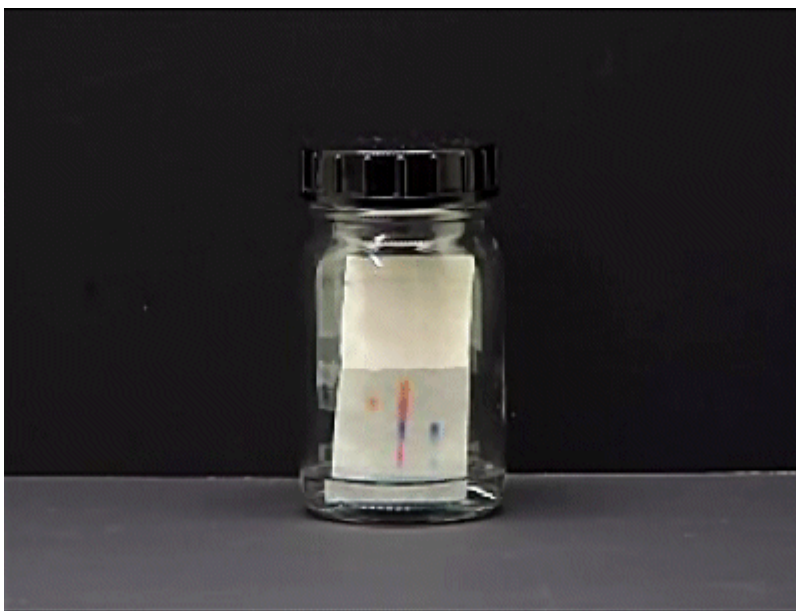


Figure 3-1: Example of Thin Layer Chromatography<sup>18</sup>

After the reaction is determined to be complete by TLC, the product was checked using a 250 MHz Nuclear Magnetic Resonance (NMR) spectrometer. An image of a typical NMR machine can be seen in Figure 3-2.<sup>19</sup> Deuterated chloroform,  $\text{CDCl}_3$ , with a known residual peak of 7.26 is used as the solvent for the NMR. The solvent is purchased from Aldrich and is not purified further before use. The correct values for the peaks in the NMR of each product are obtained from an article published by Reddy et al.<sup>8</sup>



Figure 3-2: Example of a typical NMR instrument<sup>19</sup>

In order to determine the success of the deuterated synthesis, one needs to calculate the percent of deuteriums that have replaced hydrogens in the compound. This value is calculated by taking the integral of methyl protons (twelve in this case) versus aromatic ring protons (two in this case) as seen on the NMR. These protons can be seen in the compounds in Figure 3-3, and the NMR for this precursor to the deuterated Finland trityl radical (compound 3) can be seen in Figure 3-4. For the calculation of percent deuteration of compound 3 in Figure 3-3, one needs to know the values of the peaks in the NMR. The NMR of Attempt 3 had a peak at 1.819 nm<sup>-1</sup> of 1 and a peak at 6.999 of 2.08. The percent of non-deuterated compound is calculated as  $\left(\frac{1}{2.08 \cdot 6}\right) \cdot 100$ , which is equal to about 8%. The percent of deuterated product is, therefore, 92% (100-8).

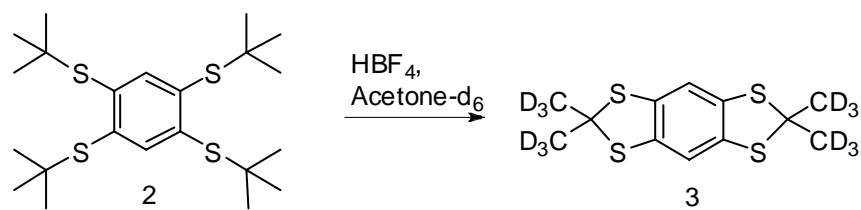


Figure 3-3: Second step in the synthesis of the deuterated trityl radical

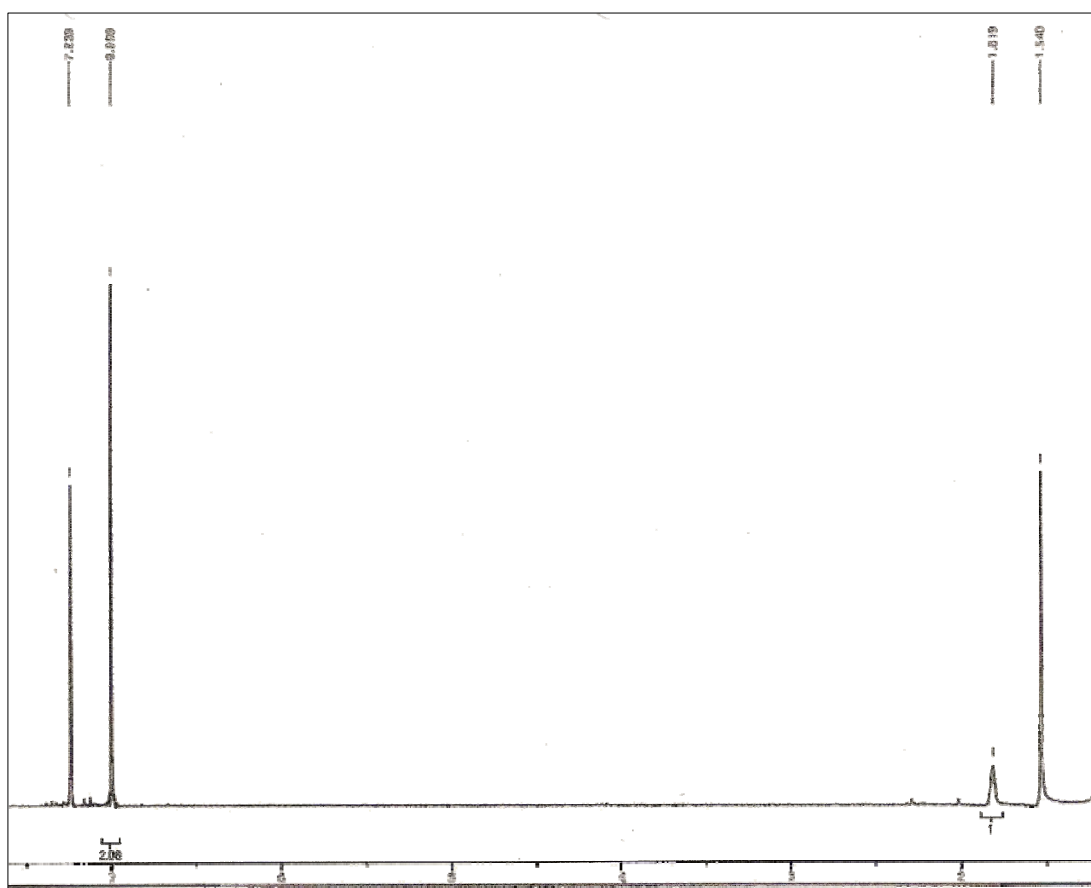


Figure 3-4: NMR of a precursor to the deuterated Finland trityl radical.



## Works Cited

1. Krishna, M., Devasahayam, N., Cook, J. A., Subramanian, S., Kuppusamy, P., & Mitchell, J. B. (2001). Electron Paramagnetic Resonance for Small Animal Imaging Applications. *ILAR Journal*, 42-3, 209-218.
2. Stith, Kevin. (Aug 2008). *Brain MRI*. Retrieved October 31<sup>st</sup>, 2008, from <http://amazinghumanbrain.blogspot.com/2008/08/brain-mri.html>
3. Afeworki, Mobae. (2000). Three-Dimensional Whole Body Imaging of Spin Probes in Mice by Time-Domain Radiofrequency Electron Paramagnetic Resonance. *Magnetic Resonance in Medicine*, 43, 375-382.
4. Beardsley, Sandra. (Summer 2009). *My Journey Living with a Brain Tumor: Sandy's Brain Tumor*. Retrieved October 31<sup>st</sup>, 2008, from [http://www.sandybeardsley.com/sandys\\_mri.html](http://www.sandybeardsley.com/sandys_mri.html)
5. Kuppusamy, Periannan, & Zweier, Jay L. (2004). Cardiac applications of EPR imaging. *NMR Biomed*, 17, 226-239.
6. Liu, S., Timmins, G. S., Shi, H., Gasparovic, C. M., & Liu, K. J. (2004). Application of in vivo EPR in brain research: monitoring tissue oxygenation, blood flow, and oxidative stress. *NMR Biomed.*, 17, 327-334.
7. Rizzi, C., Samouilov, A., Kutala, V. K., Parinandi, N. L., Zweier, J. L., & Kuppusamy, P. (2003). Application of a Trityl-Based Radical Probe for Measuring Superoxide. *Free Radical Biology & Medicine*, 35:12, 1608-1618.
8. Reddy, T. J., Iwama, T., Halpern, H. J., & Rawal, V. H. (2002). General Synthesis of Persistent Trityl Radicals for EPR Imaging of Biological Systems. *J. Org. Chem.*, 67:14, 4635-4639.
9. Xia, S., Villamena, F. A., Hadad, C. M., Kuppusamy, P., Li, Y., Zhu, H., et al. (2006). Reactivity of Molecular Oxygen with Ethoxycarbonyl Derivatives of Tetrathiatriarylmethyl Radicals. *J. Org. Chem.*, 71, 7268-7279.
10. Dhimitruka, I., Velayutham, M., Bobko, A. A., Khramtsov, V. V., Villamena, F. A., Hadad, C. M., et al. (2007). Large-scale synthesis of a persistent trityl radical for use in biomedical EPR applications and imaging. *I Bioorg. Med. Chem. Lett.*, 17, 6801-6805.

11. Driesschaert, B., Charlier, N., Gallez, B., & Marchand-Brynaert. (2008). Synthesis of two persistent fluorinated tetrathiatriarylmethyl (TAM) radicals for biomedical EPR applications. *Bioorganic & Medicinal Chemistry Letters*, 18, 4291-4293.
12. Wilson, David F. (2008). Quantifying the role of oxygen pressure in tissue function. *Am J Physiol Heart Circ Physiol*, 294, H11-13.
13. Hadad, Christopher M. Biodistribution of Bioscavengers by Electron Paramagnetic Resonance Imaging.
14. Brown, J. M., & Wilson, W. R. (2004). Exploiting tumour hypoxia in cancer treatment. *Nature Reviews Cancer*, 4, 437-447.
15. Li, H., Deng, Y., He, G., Kuppusamy, P., Lurie, D. J., & Zweier, J. L. (2002). Proton Electron Double Resonance Imaging of the In Vivo Distribution and Clearance of a Triaryl Methyl Radical in Mice. *Magnetic Resonance in Medicine*, 48, 530-534.
16. Youngde, W., Lurie, D. J., & Foster, M. A. (2002). Rapid imaging of free radicals in vivo using hybrid FISP field-cycled PEDRI. *Phys. Med. Biol*, 47, 1091-1100.
17. Liebgott, T., Li, H., Deng, Y., & Zweier, J. L. (2003). Proton Electron Double Resonance Imaging (PEDRI) of the Isolated Beating Rat Heart. *Magnetic Resonance in Medicine*, 50, 391-399.
18. Keusch, Peter. (May 2003). Separation of Food Dyes by Thin Layer Chromatography (TLC). Retrieved March 28<sup>th</sup>, 2009, from [http://www.uni-r.de/Fakultaeten/nat\\_Fak\\_IV/Organische\\_Chemie/Didaktik/Keusch/D-TLC\\_food\\_dyes-e.htm](http://www.uni-r.de/Fakultaeten/nat_Fak_IV/Organische_Chemie/Didaktik/Keusch/D-TLC_food_dyes-e.htm)
19. Yang Research Group. The University of Arizona College of Pharmacy. (May 2003). Retrieved March 28<sup>th</sup>, 2009, from <http://www.pharmacy.arizona.edu/faculty/yanlab/>